European Journal of Medicinal Chemistry 48 (2012) 244–254

Contents lists available at SciVerse ScienceDirect

European Journal of Medicinal Chemistry

journal homepage: http://www.elsevier.com/locate/ejmech

Original article

Synthesis and bioevaluation of novel 3,4,5-trimethoxybenzylbenzimidazole derivatives that inhibit *Helicobacter pylori*-induced pathogenesis in human gastric epithelial cells

Chih-Shiang Chang [a], Ju-Fang Liu [a], Hwai-Jeng Lin [b], Chia-Der Lin [c,d], Chih-Hsin Tang [c], Dah-Yuu Lu [e], Yu-Ting Sing [c], Li-Yu Chen [c], Min-Chuan Kao [c], Sheng-Chu Kuo [a], Chih-Ho Lai [c,f,g,*]

[a] *Graduate Institute of Pharmaceutical Chemistry, China Medical University, Taichung, Taiwan*
[b] *Division of Gastroenterology and Hepatology, Taipei Medical University Hospital, Taipei, Taiwan*
[c] *School of Medicine and Graduate Institute of Basic Science, China Medical University, No. 91 Hsueh-Shih Road, Taichung 40402, Taiwan*
[d] *Department of Otolaryngology, China Medical University Hospital, Taichung, Taiwan*
[e] *Graduate Institute of Neural and Cognitive Sciences, China Medical University, Taichung, Taiwan*
[f] *Department of Urology, University of Texas Southwestern Medical Center, Harry Hines Blvd., Dallas, TX 75390, USA*
[g] *Department of Life Science, National Tsing Hua University, Hsinchu, Taiwan*

ARTICLE INFO

Article history:
Received 1 August 2011
Received in revised form
16 November 2011
Accepted 13 December 2011
Available online 22 December 2011

Keywords:
Benzimidazole
Helicobacter pylori
Antibiotic resistant
Human gastric epithelial cells
Interleukin-8
2-Fluorophenyl-5-methyl-1-(3,4,5-trimethoxybenzyl)benzimidazole

ABSTRACT

Helicobacter pylori infection is associated with gastritis, peptic ulcer, and even gastric malignancy. *H. pylori*'s antibiotic resistance is the major obstacle preventing its eradication. A series of 3,4,5-trimethoxybenzylbenzimidazole derivatives were synthesized and evaluated for their anti-*H. pylori* activity. The compound, 2-fluorophenyl-5-methyl-1-(3,4,5-trimethoxybenzyl)benzimidazole (FMTMB), was determined as the most potent in the inhibition of *H. pylori* growth and pathogenesis of host cells. An *in vitro H. pylori* infection model revealed that FMTMB inhibited *H. pylori* adhesion and invasion of gastric epithelial cells. Results from this study provide evidence that FMTMB is a potent therapeutic agent that exhibits both anti-*H. pylori* growth properties and anti-*H. pylori*-induced pathogenesis of cells.

1. Introduction

Helicobacter pylori is a gram-negative bacterium that causes persistent infection in humans [1,2]. A strong correlation between *H. pylori* infection and gastrointestinal disease has been consistently reported [3], and a relatively high proportion of *H. pylori*-infected patients are at risk of development of gastritis, peptic ulcers, and even gastric cancer [4,5].

Eradication of *H. pylori* improves ulcer healing and reduces the recurrence of peptic ulcers [6,7]. Treatment of patients with a proton pump inhibitor (PPI) combined with two different antibiotics (principally clarithromycin, and amoxicillin or metronidazole) was commonly used in *H. pylori*-infected patients [8,9]. However, because of widespread use of those antibiotics during past decades, *H. pylori* antimicrobial resistance rates have been high, leading to main cause of therapy failure of *H. pylori* infection [10–12]. Therefore, we urgently require the development of novel effective compounds for alternative therapeutic approaches for controlling resistant *H. pylori* and associated diseases.

Benzimidazoles (BIs) were commonly used as PPIs to control stomach hyperacidity and also have activity against *H. pylori* growth [13]. Several BIs have been characterized as having potent

Abbreviations: PPI, proton pump inhibitor; BIs, benzimidazoles; TMB, 3,4,5-trimethoxybenzylbenzimidazole; FMTMB, 2-fluorophenyl-5-methyl-1-(3,4,5-trimethoxybenzyl)benzimidazole; MBC, minimum bactericidal concentration; VacA, vacuolating cytotoxin A; CagA, cytotoxin-associated gene A; PPTMB, 2-phenyl-5-(pyrrolidin-1-yl)-1-(3,4,5-trimethoxybenzyl)-1*H*-benzimidazole; MIC, minimal inhibition concentration.

* Corresponding author. School of Medicine and Graduate Institute of Basic Science, China Medical University, No. 91 Hsueh-Shih Road, Taichung 40402, Taiwan. Tel.: +886 4 22052121x7729; fax: +886 4 22333641.
E-mail addresses: chl@mail.cmu.edu.tw, Chih-Ho.Lai@UTSouthwestern.edu (C.-H. Lai).

0223-5234/$ – see front matter © 2011 Elsevier Masson SAS. All rights reserved.
doi:10.1016/j.ejmech.2011.12.021

and selective activities against not only *H. pylori*, but also against commensal and pathogenic microorganisms [14]. A previous study demonstrated BI's potent anti-*H. pylori* activity in animals [15]. However, *nuoD* (NADH:ubiquinone oxidoreductase), responsible for BIs resistance, was found in spontaneous *H. pylori* mutants resistant to BIs [16]. Thus, BI derivatives not only exhibit multidrug-resistant *H. pylori* activity, but might also prove effective in the inhibition of *H. pylori*-induced pathogenesis of gastric epithelial cells. We identified several BI derivatives with potent anti-*H. pylori* activity. We also determined the derivative with the greatest potency for curbing the growth of multidrug-resistant *H. pylori* and for the inhibition of *H. pylori*-induced pathogenesis in gastric epithelial cells.

2. Chemistry

The synthesis of substituted 3,4,5-trimethoxybenzylbenzimidazole (TMB) is outlined in Scheme 1. To introduce a series of substitutions at positions 5 and 6 of the benzimidazole ring, the substituted *o*-nitroaniline was used as starting material. *o*-Nitroaniline **1** was treated with an appropriate acyl chloride **2** to obtain the corresponding amide **3**. Reduction of the nitro moiety of compound **3** using iron powder or sodium dithionite as reductive agent afforded amine **4**. Iminization of **4** with 3,4,5-trimethoxybenzaldehyde in methanol then gives the Schiff-base **5**. The targets **7**–**34** as shown in Table 1 were obtained by reduction of the appropriate **5** by treatment with $NaBH_4$ in methanol, to provide **6**, followed by cyclization to furnish the final products.

3. Results

3.1. Growth inhibition of H. pylori strains

The synthesized TMBs were evaluated for *H. pylori* growth inhibitory activity, and results are shown in Table 1. Inhibition was assessed using the agar disk diffusion method, by measuring the diameter of the inhibition zone in an agar dish of concentration 100 μg/mL. The results from compounds **7** to **13** show that the introduction of an electron donating methyl group at positions 5 or 6 of the TMB core provided greater activity than compounds with electron withdrawing Cl and F groups at those positions. However, substitution with the strongly electron donating OCH_3 group dramatically reduced antimicrobial activity. Results from compounds **14**–**17** indicate that the presence of a methyl group at position-5 of the TMB core produced greater activity than methyl substitution at position-6. A variety of 5-methyl substituted TMB derivatives were synthesized (**18**–**34**). The results show that the introduction of more bulky groups at the 2-position led to compounds with reduced or little activity (**27**–**32**), and substitution at the 3′-postion of the aromatic ring resulted in inactive compounds (**20** and **22**). However, compounds **23**, **25**, **26**, and **34** exhibited good activity against *H. pylori in vitro* assay.

Among the tested TMBs, compounds **8**, **11**, **14**, **23**, **25**, **26**, and **34** exhibited significant potency with inhibition zones ranging from 21 to 24 mm (Table 1). These results are much better than the performance of the standard antimicrobial agent benzimidazole (BI). Thus, TMB derivatives, in particular compounds **26** and **34**, may be useful in the development of novel therapeutic agents targeting *H. pylori* growth.

We performed determinations to assess cell viability using the MTT method with untreated cells, and test sample-treated AGS cells. Our results showed that several compounds (**8**, **11**, **14**, **23**, **25**, **26** and **34**) possessed higher anti-*H. pylori* activity; however, they also had a potent influence on cell viability. Only derived compound **26**, 2-fluorophenyl-5-methyl-1-(3,4,5-trimethoxybenzyl) benzimidazole (FMTMB), had no influence on AGS cell growth (data not shown). Therefore, FMTMB with a maximal concentration of 20 μg/mL was chosen to examine its biological effect on the inhibition of *H. pylori*-induced pathogenesis of AGS cells.

3.2. Minimum bactericidal concentration (MBC) of FMTMB against H. pylori multidrug-resistant isolates

We assessed FMTMBs minimum bactericidal concentration (MBC) against *H. pylori* reference strain (26695) and multidrug-resistant isolates, v633 and v1254. As shown in Table 2, at pH 7.0, the MBC value for FMTMB was 25, 12.5, and 12.5 μg/mL, determined for *H. pylori* strains 26695, v633, and v1254, respectively. It was interesting to observe that the effect of buffering pH (5.0, 7.0, and 8.0) did not influence FMTMB bactericidal activity. This indicated that FMTMB harbors superior bactericidal activity against both antibiotic-susceptible and multidrug-resistant strains of *H. pylori*, and maintains its bactericidal activity over the range pH 5.0–8.0.

3.3. Inhibition of H. pylori adhesion to and invasion into AGS cells

The adhesion of *H. pylori* to gastric epithelial cells is an important initial step in the induction of host cell pathogenesis [17]. Since we determined FMTMB to have an effective level of bactericidal

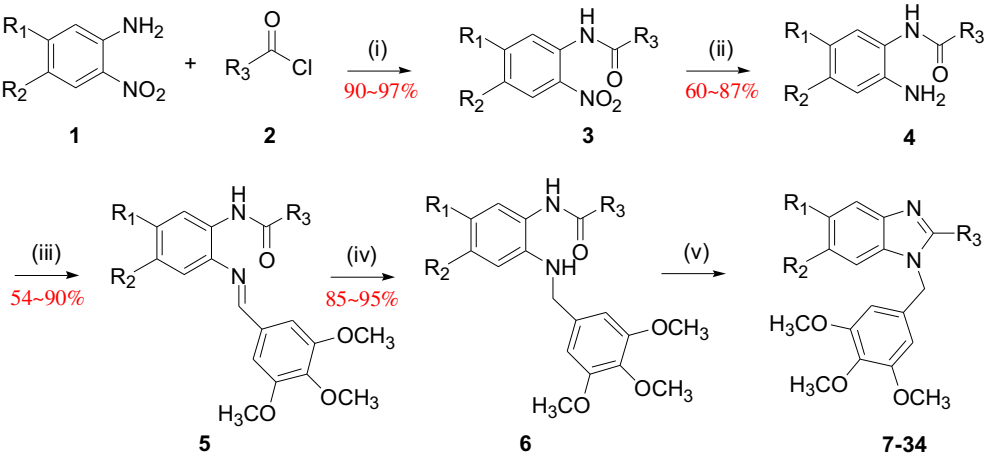

Scheme 1. Synthesis of trimethoxybenzylbenzimidazole derivatives. Reagents and conditions: (i) pyridine, CH_2Cl_2, rt; (ii) Fe, NH_4Cl, IPA, 100 °C; or $Na_2S_2O_4$, ethanol, reflux; (iii) 3,4,5-trimethoxybenzaldehyde, MeOH, rt; (iv) $NaBH_4$, MeOH; (v) MeOH/4N HCl (2:1), 50 °C.

Table 1
Chemical structures of benzimidazole derivatives and their inhibitory effect on *H. pylori* 26695 (ATCC 700392) growth during the disk agar diffusion test.

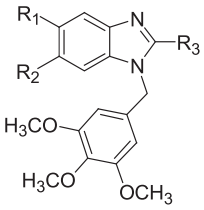

Compound[a]	Chemical formula	R1	R2	R3	Inhibition zone (mm)
7	$C_{25}H_{26}N_2O_3$	CH_3	CH_3	Ph	16
8	$C_{24}H_{24}N_2O_3$	CH_3	H	Ph	22
9	$C_{23}H_{21}ClN_2O_3$	Cl	H	Ph	11
10	$C_{23}H_{21}FN_2O_3$	F	H	Ph	17
11	$C_{24}H_{24}N_2O_3$	H	CH_3	Ph	21
12	$C_{24}H_{24}N_2O_4$	H	OCH_3	Ph	0
13	$C_{23}H_{21}ClN_2O_3$	H	Cl	Ph	14
14	$C_{25}H_{26}N_2O_4$	CH_3	H	4-OCH_3–Ph	22
15	$C_{24}H_{23}ClN_2O_4$	Cl	H	4-OCH_3–Ph	11
16	$C_{25}H_{26}N_2O_4$	H	CH_3	4-OCH_3–Ph	15
17	$C_{24}H_{23}ClN_2O_4$	H	Cl	4-OCH_3–Ph	12
18	$C_{25}H_{23}N_3O_3$	CH_3	H	4-CN–Ph	12
19	$C_{24}H_{23}FN_2O_3$	CH_3	H	4-F–Ph	17
20	$C_{25}H_{26}N_2O_4$	CH_3	H	3-OCH_3–Ph	0
21	$C_{25}H_{26}N_2O_3$	CH_3	H	3-CH_3–Ph	19
22	$C_{24}H_{23}FN_2O_3$	CH_3	H	3-F–Ph	0
23	$C_{25}H_{26}N_2O_4$	CH_3	H	2-OCH_3–Ph	21
24	$C_{25}H_{26}N_2O_3$	CH_3	H	2-CH_3–Ph	14
25	$C_{24}H_{23}ClN_2O_3$	CH_3	H	2-Cl–Ph	21
26 (FMTMB)	$C_{24}H_{23}FN_2O_3$	CH_3	H	2-F–Ph	24
27	$C_{28}H_{26}N_2O_3$	CH_3	H	1-Naphthyl	12
28	$C_{28}H_{26}N_2O_3$	CH_3	H	2-Naphthyl	0
29	$C_{26}H_{26}N_2O_3$	CH_3	H	Styryl	15
30	$C_{24}H_{22}Cl_2N_2O_3$	CH_3	H	3,4-diCl–Ph	9
31	$C_{24}H_{22}Cl_2N_2O_3$	CH_3	H	2,4-diCl–Ph	11
32	$C_{24}H_{22}Cl_2N_2O_3$	CH_3	H	2,3-diCl–Ph	13
33	$C_{24}H_{22}F_2N_2O_3$	CH_3	H	2,5-diF–Ph	11
34	$C_{24}H_{22}F_2N_2O_3$	CH_3	H	2,6-diF–Ph	24
BI	$C_7H_6N_2$				0
AMX					14
CLR					21
MTZ					7

[a] FMTMB: 2-fluorophenyl-5-methyl-1-(3,4,5-trimethoxybenzyl)benzimidazole, BI: benzimidazole, AMX: amoxicillin, CLR: clarithromycin, and MTZ: metronidazole. Concentration of compounds **7**–**34** was at 100 μg/mL, BI at 100 μg/mL, AMX and CLR at 50 μg/mL, and MTZ at 800 μg/mL. DMSO was used as a negative control.

activity, we further examined whether it is able to inhibit the initial step of *H. pylori* adhesion to, and invasion of host cells. As shown in Fig. 1A, FMTMB exhibited dramatic inhibition activity against *H. pylori* adhesion to AGS cells by 6%, 31%, and 58% at 5, 10, and 20 μg/mL respectively, as compared with the DMSO control.

Table 2
Effect of pH on minimum bactericidal concentration (MBC) of FMTMB against *H. pylori* 26695, and multidrug-resistant strains v633 and v1354.

H. pylori strains	Tested compound[a]								
	MTZ			BI			FMTMB		
	pH			PH			pH		
	5.0	7.0	8.0	5.0	7.0	8.0	5.0	7.0	8.0
26695	6.25	12.5	12.5	>800	400	>800	25	25	25
v633	50	50	50	>800	400	400	12.5	12.5	12.5
v1254	100	100	100	>800	400	400	12.5	12.5	12.5

[a] AMX: amoxicillin, BI: Benzimidazole, FMTMB: 2-fluorophenyl-5-methyl-1-(3,4,5-trimethoxybenzyl)benzimidazole. Concentrations of FMTMB and standard antimicrobial agents were in μg/mL.

Additionally, FMTMB showed significant anti-invasion activity against *H. pylori*, with a reduction of 7%, 28%, and 52% in concentrations of 5, 10, and, 20 μg/mL (Fig. 1B). On the other hand, DMSO had no effect either adhesion or invasion activities of *H. pylori*. Standard antibiotic MTZ (20 μg/mL) only produced only a slight inhibitory effect (~20%) in anti-adhesion and anti-invasion assays, indicating that at the same concentration of 20 μg/mL, FMTMB is more effective than the standard drug MTZ in inhibition of *H. pylori* adhesion to, and invasion of, AGS cells. Results from this data demonstrate that the BI derivative FMTMB, exhibited not only bactericidal activity, but also provides related anti-adhesion and anti-invasion activities.

3.4. Inhibitory effects of H. pylori-induced vacuolation in AGS cells

H. pylori vacuolating cytotoxin A (VacA) induces formation of vacuoles, which causes continuous cell swelling that can eventually

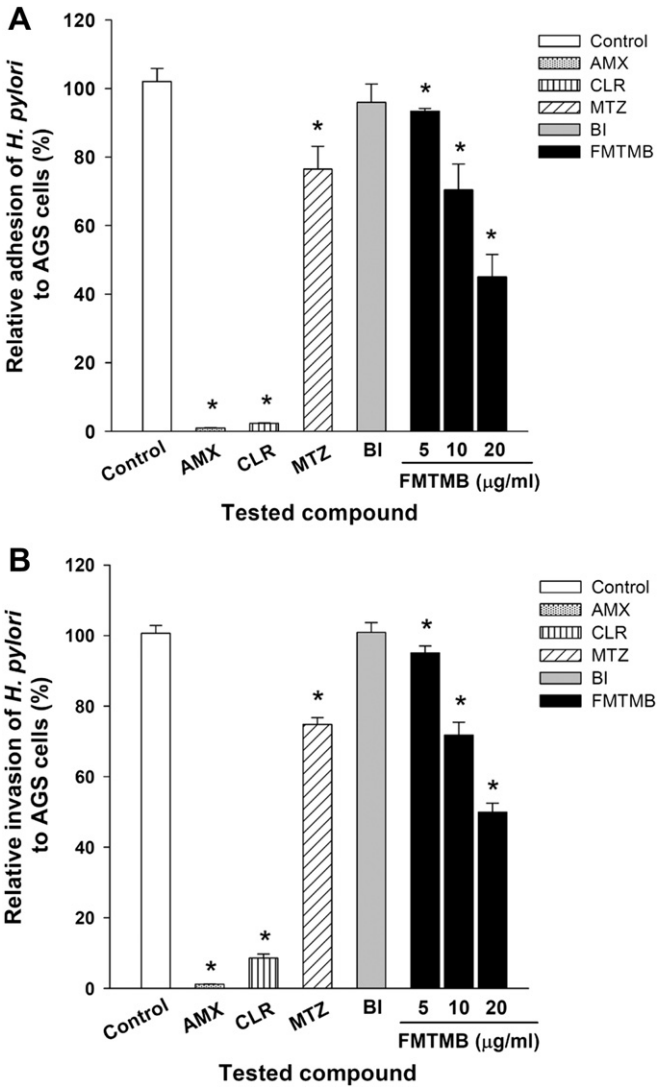

Fig. 1. Effects of FMTMB and standard antimicrobial agents on *H. pylori* adhesion (A) and invasion (B) to gastric epithelial cells. AGS cells were treated with FMTMB and antimicrobial agents, followed by incubation with *H. pylori* at MOI 50 for 6 h. Amoxicillin (AMX), clarithromycin (CLR), metronidazole (MTZ), and benzimidazole (BI) were used as positive control antimicrobial agents. Each experiment result shown represents mean values ± the standard deviation of three independent experiments. Statistical analysis was calculated using Student's *t*-test when compared to DMSO treated cells. $^*P < 0.05$ was considered as statistically significant.

lead to cell death by necrosis [18]. We sought to assess whether FMTMB was able to inhibit *H. pylori* VacA-induced vacuolation activity. A standard neutral red uptake assay was employed for the detection of AGS cell vacuolation [19]. The assay showed that AGS cells infected with *H. pylori* accumulate significantly more dye than un-infected cells (Fig. 2). Compared to the control, addition of BI showed poor inhibition of *H. pylori*-induced vacuole formation of cells. However, after pretreatment of FMTMB, we observed a concentration-dependent inhibition of neutral red uptake (Fig. 2). This suggests that FMTMB has the ability to inhibit *H. pylori*-induced vacuolation in gastric epithelial cells.

3.5. Inhibitory effects of H. pylori-induced inflammation of AGS cells

H. pylori adherence to AGS cells induces translocation and phosphorylation of cytotoxin-associated gene A (CagA) [20]. A previous study demonstrated the translocation and phosphorylation of CagA in gastric epithelial cells, resulting in the activation of NF-κB, followed by activation of IL-8 transcription and induction of hummingbird phenotype formation, indicating that *H. pylori* CagA plays an important role in inducing IL-8 secretion [21]. Thus, we intended to investigate whether FMTMB reduces the extent of *H. pylori* CagA translocation and phosphorylation in AGS cells. CagA was immunoprecipitated from *H. pylori*-infected cells and analyzed by immunoblot assay to quantify the amount of CagA protein delivered into AGS cells. As shown in Fig. 3A, both the levels of translocated and tyrosine-phosphorylated CagA decreased in a concentration-dependent manner upon pretreatment of *H. pylori*-infected cells with various concentrations of FMTMB (0–20 μg/mL). Compared with non-treated cells, there was nearly 55% reduction in translocated CagA and tyrosine-phosphorylated CagA when *H. pylori*-infected cells were treated with 20 μg/mL of FMTMB (Fig. 3B and C). We next explored whether FMTMB, in addition to inhibit translocation and phosphorylation of CagA, also specifically attenuates CagA-induced responses by evaluating the hummingbird phenotype of AGS cells. Upon AGS cell infection by *H. pylori*, around 30% of AGS cells exhibited the hummingbird phenotype, compared to the non-treated cells (Fig. 4). With pretreatment of FMTMB, the proportion of elongated cells was reduced in a concentration-dependent manner. *H. pylori*-induced AGS elongation was dramatically reduced by 98% of the starting population when infected cells were pretreated with 20 μg/mL of FMTMB, indicating that FMTMB attenuates CagA translocation, leading to a reduction in the amount of CagA phosphorylation, and attenuating the AGS cell hummingbird phenotype. Collectively, these results indicate that FMTMB plays an important role in the reduction of *H. pylori* CagA biological functions in AGS cells.

We further analyzed whether FMTMB influences NF-κB activation. NF-κB-luc construct was used to determine luciferase expression following treatment of cells with FMTMB and co-incubation with *H. pylori*. AGS cells were transiently transfected with NF-κB-luc construct, followed by treatment with FMTMB and infected with *H. pylori*. The standard antimicrobial agent BI had only a slight inhibitory effect on the induction of NF-κB activity at a maximum concentration of 20 μg/mL as compared to the DMSO control. In contrast to BI, FMTMB exhibited significant inhibition of luciferase activity by 14 and 42% compared to the DMSO control at concentrations of 10 and 20 μg/mL, respectively (Fig. 5A). Since *H. pylori*-induced IL-8 expression of gastric epithelial cells is mediated by activation of NF-κB [21], we next measured FMTMB's inhibitory effect on *H. pylori*-induced AGS cell IL-8 expression. The secretion of IL-8 in AGS cells infected with *H. pylori* in the presence of FMTMB at concentrations ranging from 0 to 20 μg/mL was measured. In consistence with the NF-κB activity assay, IL-8 secretion in AGS cells infected with *H. pylori* was reduced by 85% upon pretreatment with 20 μg/mL of FMTMB (Fig. 5B). The results from this study indicate that suppression of IL-8 secretion by pretreatment with FMTMB might contribute to attenuation of NF-κB activity by gastric epithelial cells in response to *H. pylori* infection.

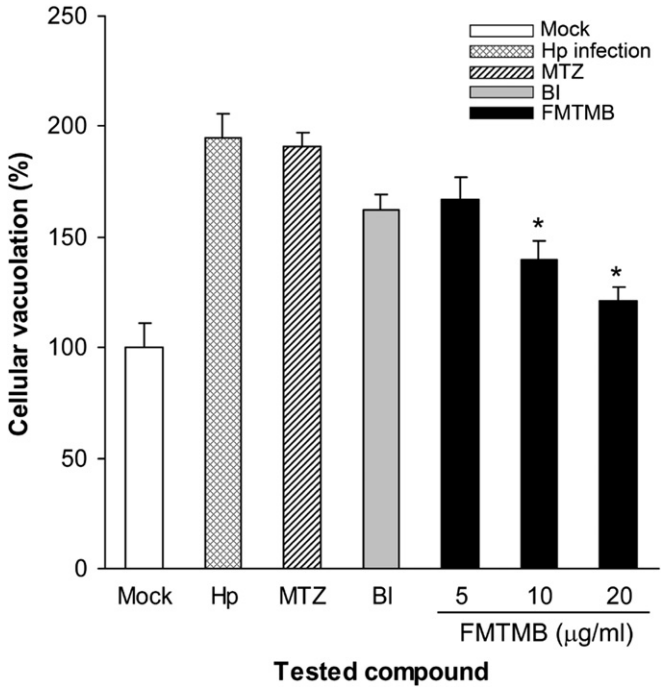

Fig. 2. FMTMB attenuates VacA-induced vacuolation of *H. pylori*-infected AGS cells. Pretreatment of *H. pylori*-infected AGS cells with BI, and various concentrations (5, 10, and 20 μg/mL) of FMTMB; the cells were cultured for 24 h and stained with 0.05% neutral red. The net OD for each well, indicating the accumulation of neutral red dye in cells, was evaluated. The control of AGS cells without *H. pylori* infection and without test sample present was used as a baseline for 100% cellular vacuolation. Results are shown as mean values ± standard deviations from three independent experiments. $^{*}P < 0.05$ was considered as significantly different.

4. Discussion

Benzimidazole derivatives are generally provided as PPIs to prevent gastric hyperacidity, and have been investigated for inhibitory effects against several microbes including *Fusobacterium nucleatum* [22], *Streptococcus mutans* [23], and *H. pylori* [15]. Target for BI, including omeprazole and lansoprazole, is gastric parietal cell proton-pumping P-ATPases and are commonly used as a part of a multiple regimen for treatment of *H. pylori*-related gastroenteritis [24]. In addition, a BI analog, 2-phenyl-5-(pyrrolidin-1-yl)-1-(3,4,5-trimethoxybenzyl)-1*H*-benzimidazole (PPTMB) was found to have anti-cancer activity by the disruption of microtubule dynamics, arresting the cell cycle and leading to stimulation of mitochondria-related apoptotic cascades in prostate cancer cells [25]. Based on these previous reports demonstrating multiple functions of benzimidazole derivatives, we synthesized a series of TMB derivatives, with the aim of developing therapeutic agents against *H. pylori* growth and associated pathogenesis. After extensive functional screening analysis of 28 derivatives, one compound, FMTMB, was clearly distinguished above the others.

Resistance to antibiotic treatment has become the most important factor in the eradication of *H. pylori* infection [26]. *H. pylori* adhesion to epithelial cells is a crucial initial step in the pathogenesis of gastric-related diseases [17]. Our previous study reported that pretreatment of *H. pylori* isolates from the failure

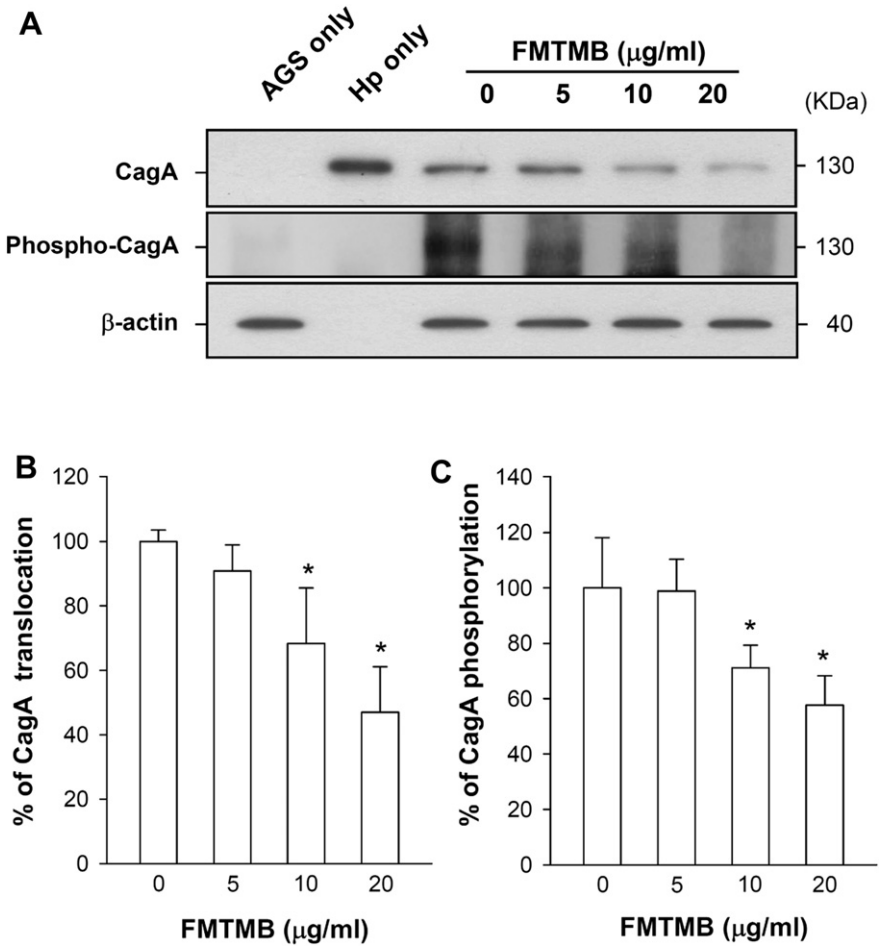

Fig. 3. The effects of FMTMB on *H. pylori* CagA translocation and phosphorylation. (A) AGS cells were treated with various concentrations of FMTMB (5, 10, and 20 μg/mL) after prior infection by *H. pylori* at MOI 100 for 6 h. After washing three times, whole-cell lysates were immunoprecipitated for CagA, and subjected to immunoblot analysis. Translocated CagA and phosphorylated CagA were stained using mouse anti-CagA and mouse anti-phosphotyrosine antibodies, respectively. β-Actin was detected using goat anti-actin antibody to represent an internal control for equal loading. The quantitative results of (B) CagA translocation and (C) CagA phosphorylation were determined using densitometric analysis. Results are shown as mean values ± standard deviations from three independent experiments. $^{*}P < 0.05$ was considered as statistically significant.

group of a clinical trial, had greater internalization activity than those from the group that were successfully eradicated [27]. These reports suggest that *H. pylori* with either high antibiotic resistance, or elevated invading activity, or both, survive better during antibiotic treatment, thus leading to persistent intracellular survival in the human stomach. Therefore, development of a new drug for inhibition of *H. pylori* invasion of host cells may be effective in the prevention of bacteria forming antibiotic resistance. In the present study, it was observed that FMTMB displayed greater anti-adhesion activity than BI did (Fig. 1A). FMTMB also showed significantly better inhibition of *H. pylori* growth, including multidrug-resistant strains from clinical isolates than that of BI. In a study of 25 aerobic bacterial strains and 18 anaerobic bacterial strains, Carcanague et al. showed that BI derivatives are highly selective for *H. pylori*, with minimal inhibition concentration (MIC) values at 90% selectivity, greater than 64 μg/mL [14]. FMTMB produced MBC values against *H. pylori* and multidrug-resistant strains ranging from 12.5 to 25 μg/mL (Table 2), which were much better than BI treatment of those strains. Additionally, FMTMB showed a dramatic reduction in *H. pylori* invasion. These results indicate that FMTMB is effective as an anti-*H. pylori* agent, in addition to its anti-adhesion and anti-invasion properties.

Two bacterial virulence factors – VacA and CagA, were previously thought closely associated with peptic ulcers, and more virulent strains of *H. pylori* were thought to express both toxins [28]. Accumulated studies have demonstrated that VacA not only contributes to *H. pylori* colonization of the stomach, but also facilitates bacterial invasion into host cells [29]. Another virulent bacterial molecule – CagA, a highly immune-dominant antigen, can be translocated and phosphorylated by gastric epithelial cells [20]. Translocation of CagA may play a crucial role in *H. pylori*-induced nuclear factor-kappaB (NF-κB) activation and IL-8 expression, which are important factors in the induction of inflammatory response [21]. Thus, we considered that development of effective agents against *H. pylori* produced virulence factors would be useful for reducing of *H. pylori*-induced pathogenesis. Among the BI derivatives, we demonstrated that FMTMB is most effective in the control of *H. pylori* VacA-induced cellular vacuolation. Additionally, FMTMB suppressed *H. pylori* CagA-induced inflammation through inhibition of CagA translocation and phosphorylation, and the pro-inflammatory signaling pathway components NF-κB and IL-8. However, the mechanisms by which FMTMB inhibits VacA and CagA remain unclear and require further investigation.

5. Conclusions

In this study, we synthesized 28 TMB derivatives and demonstrated that the most potent of these, FMTMB, is effective in the

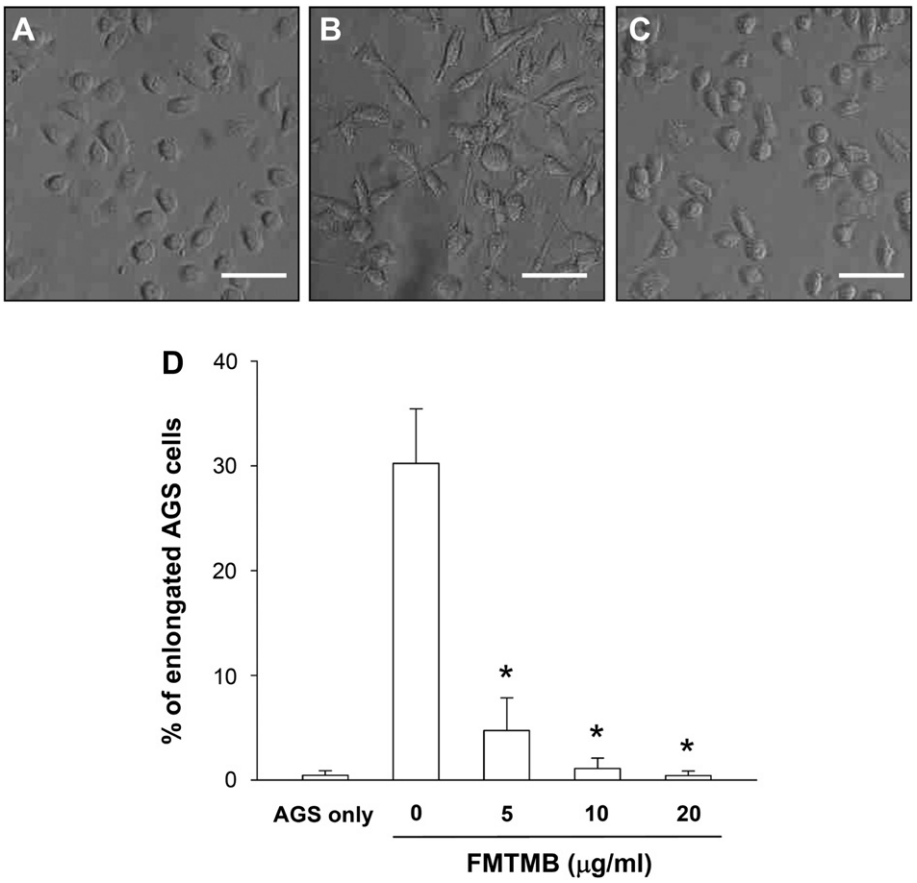

Fig. 4. Inhibitory effects of FMTMB on *H. pylori* CagA-induced pathogenesis of AGS cells. The hummingbird phenotype of *H. pylori* CagA-induced AGS cells was reduced after treatment with FMTMB. (A) Mock infection, (B) *H. pylori*-infected AGS cells, (C) pretreatment of *H. pylori*-infected AGS cells with FMTMB (20 μg/mL), followed by incubation for a further 6 h, (D) the proportion of elongated (hummingbird phenotype) cells was evaluated. Results are shown as mean values ± standard deviations from three independent experiments. Differences were considered significant for $^{*}P < 0.05$. Scale bar, 20 μm.

inhibition of *H. pylori* growth. FMTMB inhibits both *H. pylori* adhesion and invasion of gastric epithelial cells, and diminishes both bacterial-induced IL-8 secretion and NF-κB activation. Moreover, FMTMB showed activity against both *H. pylori* reference and multidrug-resistant strains. In particular, *H. pylori*-induced pathogenesis, which is enhanced by CagA and VacA, showed a dramatic reduction after by treatment of cells with FMTMB. Thus, this study showed that FMTMB has the potential to be a new potent

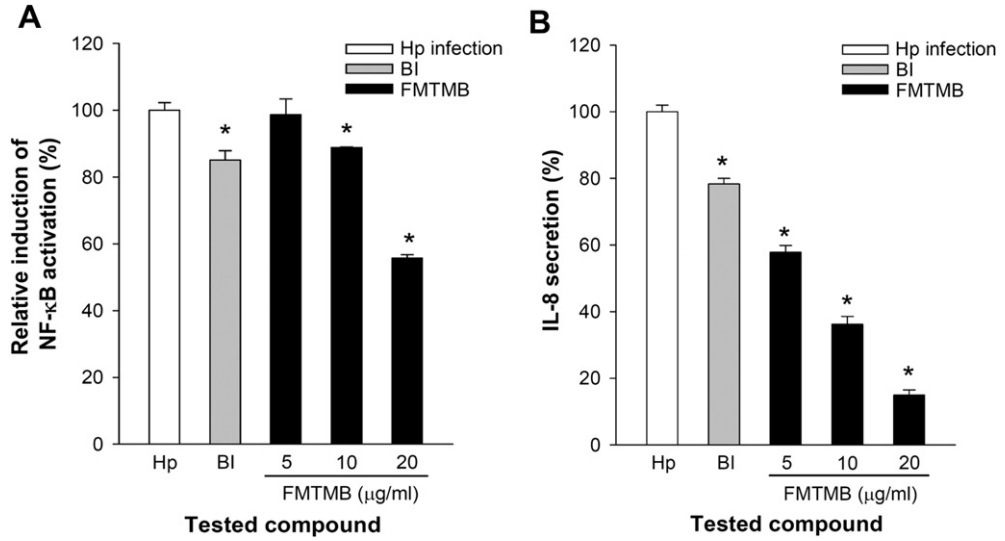

Fig. 5. The effects of FMTMB on *H. pylori*-induced AGS cells inflammatory response. FMTMB inhibits (A) NF-κB activation and (B) IL-8 expression. Benzimidazole (BI) (20 μg/mL) was used as a control standard antimicrobial agent. We determined luciferase activity and IL-8 secretion in the culture supernatants. Results are shown as mean values ± standard deviations from three independent experiments. Statistical significance was calculated using the Student's *t*-test when compared to the DMSO control. $^{*}P < 0.05$ was considered as statistically significant.

therapeutic drug against *H. pylori* infection and inflammation of gastric epithelial cells.

6. Experimental section

6.1. Chemistry

6.1.1. General experimental procedures

Reagents and solvents were obtained commercially and used without further purification. Reactions were monitored by TLC, using Merck plates with fluorescent indicator (TLC Silica Gel 60 F_{254}). Flash column chromatography was performed on silica gel (Merck Silica Gel 60, 70–230 mesh). Melting points were determined on a Yanaco MP-500D melting point apparatus and were uncorrected. ^{1}H and ^{13}C NMR spectra were obtained on a Bruker NMR AV 400 or DPX-200 spectrometer in DMSO-d_6 or $CDCl_3$-d_1. The following abbreviations are used: s, singlet; d, doublet; t, triplet; m, multiplet. EIMS and HRMS spectra were measured with a Finnigan/Thermo Quest MAT95×l instrument. ESIMS spectra were measured with a Bruker esquire HCT ultra instrument. All the synthetic benzimidazole derivatives, with the exception of compound **10**, were checked by elemental analysis. Elemental analyses (C, H, and N) were performed on an Elementar vario EL III analyzer, and the results were within ±0.4% of the calculated values. The purity of the oil compound **10** was checked by Jasco HPLC analysis possessed more than 99% purity.

6.1.2. N-(Substituted-2-nitrophenyl)benzamides (*3*)

To a stirred solution of substituted 2-nitroaniline (4 mmol) and pyridine (8 mmol) in dry dichloromethane (15 mL) was added dropwise the corresponding benzoyl chloride (8 mmol). The reaction mixture was stirred at room temperature for 8 h. The solvent was evaporated *in vacuo*, and the residue subjected to flash chromatography on silica gel using a mixture of hexanes–CH_2Cl_2 (7:3) as eluent which after drying *in vacuo*, afforded **3** as a solid.

6.1.3. N-(2-amino-substituted phenyl)benzamides (*4*)

To a suspension of compound **3** (3 mmol) in isopropanol (150 mL) was added iron powder (2 g) and ammonium chloride (0.3 mmol). The reaction mixture was heated at 100 °C for 12 h. The hot mixture was filtered off and the filtrate was evaporated. The residue was subjected to flash chromatography on silica gel using a mixture of hexanes–CH_2Cl_2 (9:1) as eluent which after drying *in vacuo*, afforded **4** as a white-gray solid.

6.1.4. N-(Substituted-2-(3,4,5-trimethoxybenzylidenamino)phenyl) benzamides (*5*)

A mixture of compound **4** (2 mmol) and 3,4,5-trimethoxybenzaldehyde (3 mmol) in methanol was stirred at room temperature for 12 h. The suspension was filtered and the solid washed with methanol to afford **5** as a solid.

6.1.5. N-(Substituted-2-(3,4,5-trimethoxybenzylamino)phenyl) benzamides (*6*)

A suspension of compound **5** (3 mmol) in methanol was cooled with vigorous stirring while cooled in an ice bath. Sodium borohydride was added dropwise until the color of the mixture became white. Excess sodium borohydride was quenched by the addition of distilled water. The resulting mixture was extracted with ethyl acetate (3 × 50 mL). The combined organic components were washed with brine, dried over anhydrous $MgSO_4$, and concentrated *in vacuo* to obtain **6** as a solid.

6.1.6. Substituted-2-phenyl-1-(3,4,5-trimethoxybenzyl) benzimidazoles (*7*–*34*)

To a suspension of **6** (1 mmol) in ethanol (20 mL) was added 3 mL of 4 N HCl. The suspension was heated with vigorous stirring at 50 °C for 5 h. After cooling, the reaction solution was neutralized with ammonium hydroxide, and the resulting mixture was extracted with ethyl acetate (3 × 50 mL). The combined organic components were washed with brine, dried over anhydrous $MgSO_4$, and concentrated *in vacuo*. The residue was subjected to flash chromatography on silica gel to obtain corresponding target as a solid.

6.1.7. 5,6-Dimethyl-2-phenyl-1-(3,4,5-trimethoxybenzyl) benzimidazole (*7*)

Yield 66% from **6** as a white solid, mp 146–147 °C; ^{1}H NMR (400 MHz, DMSO-d_6) δ (ppm): 7.75–7.72 (m, 2H, ArH), 7.53–7.52 (m, 3H, ArH), 7.46 (s, 1H, ArH), 7.34 (s, 1H, ArH), 6.28 (s, 2H, ArH), 5.42 (s, 2H, CH_2), 3.57 (s, 3H, OCH_3), 3.57 (s, 6H, OCH_3), 2.31 (s, 6H, CH_3); ^{13}C NMR (100 MHz, DMSO-d_6) δ (ppm): 160.5, 153.5, 153.5, 141.8, 137.2, 134.9, 133.1, 131.8, 130.0, 130.0, 130.0, 130.0, 129.5, 129.3, 119.8, 111.5, 104.2, 104.2, 60.4, 56.2, 56.2, 47.9, 21.4, 21.4, 21.4; EIMS: *m*/*z* 402 (M^+); Anal. Calcd for $C_{25}H_{26}N_2O_3$: C, 74.60; H, 6.51; N, 6.96. Found: C, 74.41; H, 6.71; N, 6.70.

6.1.8. 5-Methyl-2-phenyl-1-(3,4,5-trimethoxybenzyl) benzimidazole (*8*)

Yield 89% from **6** as a white solid, mp 133–134 °C; ^{1}H NMR (400 MHz, DMSO-d_6) δ (ppm): 7.83–7.79 (m, 3H, 4, 2′, 6′-H), 7.48–7.37 (m, 4H, 7, 3′, 4′, 5′-H), 7.07 (dd, J = 8, 2 Hz, 1H, 6H), 6.29 (s, 2H, 2″, 6″-H), 5.34 (s, 2H, CH_2), 3.57 (s, 3H, OCH_3), 3.57 (s, 6H, OCH_3), 2.40 (s, 3H, CH_3); ^{13}C NMR (100 MHz, DMSO-d_6) δ (ppm): 164.6, 162.1, 153.5, 153.5, 152.8, 143.4, 137.1, 134.5, 133.0, 131.9, 131.9, 127.4, 124.6, 119.5, 116.3, 119.6, 111.2, 104.1, 104.1, 60.4, 56.2, 56.2, 48.0, 21.6; EIMS: *m*/*z* 388 (M^+); Anal. Calcd for $C_{24}H_{24}N_2O_3$: C, 74.21; H, 6.23; N, 7.21. Found: C, 74.15; H, 6.50; N, 7.14.

6.1.9. 5-Chloro-1-(3,4,5-trimethoxyphenyl)benzimidazole (*9*)

Yield 85% from **6** as a pale-yellow solid, mp 122–123 °C; ^{1}H NMR (400 MHz, DMSO-d_6) δ (ppm): 7.78–7.76 (m, 3H, ArH), 7.64 (d, J = 8 Hz, 1H, ArH), 7.65–7.62 (m,3H, ArH), 7.29(dd, J = 8, 2 Hz, 1H, ArH), 6.28 (s, 2H, ArH), 5.48 (s, 2H, CH_2), 3.58 (s, 3H, OCH_3), 3.58 (s, 6H, OCH_3); ^{13}C NMR (100 MHz, DMSO-d_6) δ (ppm):154.7 153.0, 153.0, 143.4, 136.7, 134.6, 132.0, 130.0, 129.8, 129.2, 129.2, 128.8, 128.8, 126.6, 122.7, 118.6, 112.6, 103.8, 103.8, 59.8, 55.7, 55.7, 47.6; ESIMS: *m*/*z* 409 $(M + 1)^+$; Anal. Calcd for $C_{23}H_{21}ClN_2O_3$: C, 67.56; H, 5.18; N, 6.85. Found: C, 67.70; H, 5.20; N, 6.72.

6.1.10. 5-Fluoro-2-phenyl-1-(3,4,5-trimethoxybenzyl) benzimidazole (*10*)

Yield 57% from **6** as a light-brown solid; mp 102–104 °C; ^{1}H NMR (400 MHz, DMSO-d_6) δ (ppm): 7.79–7.76 (m, 2H, ArH), 7.61–7.55 (m, 3H, ArH), 7.51–7.49 (m, 1H, ArH), 7.30–7.28 (m, 1H, ArH), 7.14–7.12 (m, 1H, ArH), 6.29 (s, 2H, ArH), 5.48 (s, 2H, CH_2), 3.56 (s, 3H, OCH_3), 3.56 (s, 6H, OCH_3); ^{13}C NMR (100 MHz, DMSO-d_6) δ (ppm): 154.9, 152.9, 152.9, 136.7, 132.5, 132.1, 130.0, 129.2, 129.2, 128.8, 128.8, 112.1, 111.9, 110.9, 110.6, 104.9, 104.7, 103.8, 103.8, 59.8, 55.7, 55.7, 47.6; EIMS: *m*/*z* 392 (M^+); HRMS: *m*/*z* 392.1539.

6.1.11. 6-Methyl-2-phenyl-1-(3,4,5-trimethoxybenzyl) benzimidazole (*11*)

Yield 73% from **6** as a white solid, mp 86–93 °C; ^{1}H NMR (400 MHz, DMSO-d_6) δ (ppm): 7.76–7.73 (m, 2H, ArH), 7.58–7.53 (m, 4H, ArH), 7.38 (s, 1H, ArH), 7.08–7.05 (m, 1H, ArH), 6.28 (s, 2H, ArH), 5.44 (s, 2H, CH_2), 3.57 (s, 9H, OCH_3), 2.41 (s, 3H, CH_3); ^{13}C NMR (100 MHz, DMSO-d_6) δ (ppm): 153.0, 153.0, 152.8, 140.8, 136.7, 136.1,

132.5, 132.1, 130.4, 129.6, 129.6, 129.1, 129.1, 128.8, 123.7, 118.8, 110.7, 103.7, 103.7, 59.9, 55.7, 55.7, 47.3, 21.4; ESIMS: *m/z* 389 $(M+1)^+$; Anal. Calcd for $C_{24}H_{24}N_2O_3$: C, 74.21; H, 6.23; N, 7.21. Found: C, 74.10; H, 6.41; N, 7.11.

6.1.12. 6-Methoxy-2-phenyl-1-(3,4,5-trimethoxybenzyl) benzimidazole (**12**)

Yield 77% from **6** as a white solid, mp 105–106 °C; ^{1}H NMR (200 MHz, $CDCl_3$-d_1) δ (ppm): 7.74–7.64 (m, 3H, ArH), 7.46–7.43 (m, 3H, ArH), 6.93 (dd, $J=8$, 2 Hz, 1H, ArH), 6.70 (d, $J=2$ Hz, 1H, ArH), 6.28 (s, 2H, ArH), 5.30 (s, 2H, CH_2), 3.82 (s, 3H, OCH_3), 3.80 (s, 3H, OCH_3), 3.69 (s, 6H, OCH_3); ^{13}C NMR (50 MHz, $CDCl_3$-d_1) δ (ppm): 156.9, 153.8, 153.8, 153.8, 147.3, 137.4, 132.0, 129.7, 129.1, 129.1, 129.1, 128.8, 128.8, 128.8, 120.5, 111.6, 103.0, 103.0, 94.3, 60.9, 56.1, 56.1, 48.5, 43.3; EIMS: *m/z* 404 (M^+); Anal. Calcd for $C_{24}H_{24}N_2O_4$: C, 71.27; H, 5.98; N, 6.93. Found: C, 71.35; H, 6.01; N, 6.74.

6.1.13. 6-Chloro-2-phenyl-1-(3,4,5-trimethoxybenzyl) benzimidazole (**13**)

Yield 64% from **6** as a pale-yellow solid, mp 110–111 °C; ^{1}H NMR (400 MHz, DMSO-d_6) δ (ppm): 7.79–7.76 (m, 3H, ArH), 7.71 (d, $J=8$ Hz, 1H, ArH), 7.57–7.55 (m, 3H, ArH), 7.26 (dd, $J=8$, 2 Hz, 1H, ArH), 6.27 (s, 2H, ArH), 5.49 (s, 2H, CH_2), 3.56 (s, 3H, OCH_3), 3.56 (s, 6H, OCH_3); ^{13}C NMR (100 MHz, DMSO-d_6) δ (ppm): 154.3, 152.9, 152.9, 141.3, 136.8, 136.5, 132.0, 130.0, 129.9, 129.1, 129.1, 128.9, 128.9, 127.1, 122.5, 120.5, 111.1, 103.9, 103.9, 59.9, 55.7, 55.7, 47.5; EIMS: *m/z* 408 (M^+); Anal. Calcd for $C_{23}H_{21}ClN_2O_3$: C, 67.56; H, 5.18; N, 6.85. Found: C, 67.72; H, 5.31; N, 6.74.

6.1.14. 2-(4-Methoxyphenyl)-5-methyl-1-(3,4,5-trimethoxybenzyl) benzimidazole (**14**)

Yield 68% from **6** as a white solid, mp 185–186 °C; ^{1}H NMR (400 MHz, DMSO-d_6) δ (ppm): 7.69–7.67 (m, 2H, ArH), 7.45 (m, 1H, ArH), 7.39 (d, $J=6$ Hz, 1H, ArH), 7.09 (dd, $J=8$, 2 Hz, 2H, ArH), 7.04 (dd, $J=6$, 2 Hz, 1H, ArH), 6.29 (s, 2H, ArH), 5.41 (s, 2H, CH_2), 3.82 (s, 3H, OCH_3), 3.56 (s, 9H, OCH_3), 2.41 (s, 3H, CH_3); ^{13}C NMR (100 MHz, DMSO-d_6) δ (ppm): 160.3, 153.1, 152.9, 152.9, 142.9, 136.6, 134.0, 132.6, 131.0, 130.5, 130.5, 123.7, 122.6, 118.7, 114.2, 114.2, 110.4, 103.7, 103.7, 59.9, 55.7, 55.7, 55.2, 47.5, 21.2; EIMS: *m/z* 418 $(M)^+$; Anal. Calcd for $C_{25}H_{26}N_2O_4$: C, 71.75; H, 6.26; N, 6.69. Found: C, 71.66; H, 6.40; N, 6.58.

6.1.15. 5-Chloro-2-(4-methoxyphenyl)-1-(3,4,5-trimethoxybenzyl) benzimidazole (**15**)

Yield 86% from **6** as a pale-yellow solid, mp 116–117 °C; ^{1}H NMR (400 MHz, DMSO-d_6) δ (ppm): 7.74–7.70 (m, 3H, ArH), 7.58 (d, $J=8$ Hz, 1H, ArH), 7.25 (dd, $J=8$, 2 Hz, 1H, ArH), 7.12–7.10 (m, 2H, ArH), 6.30 (s, 2H, ArH), 5.47 (s, 2H, CH_2), 3.82 (s, 3H, OCH_3), 3.57 (s, 9H, OCH_3); ^{13}C NMR (100 MHz, DMSO-d_6) δ (ppm): 161.1, 155.3, 153.6, 153.6, 144.0, 137.3, 135.2, 132.7, 131.2, 131.2, 127.0, 122.9, 122.5, 118.9, 114.9, 114.9, 112.9, 104.3, 104.3, 60.4, 56.3, 56.3, 55.9, 48.2; EIMS: *m/z* 438 $(M)^+$; Anal. Calcd for $C_{24}H_{23}ClN_2O_4$: C, 65.68; H, 5.28; N, 6.38. Found: C, 65.54; H, 5.35; N, 6.32.

6.1.16. 2-(4-Methoxyphenyl)-6-methyl-1-(3,4,5-trimethoxybenzyl) benzimidazole (**16**)

Yield 80% from **6** as a white solid, mp 96–97 °C; ^{1}H NMR (400 MHz, DMSO-d_6) δ (ppm): 7.69–7.66 (m, 2H, ArH), 7.54 (d, $J=8$ Hz, 1H, ArH), 7.32 (s, 1H, ArH), 7.09–7.03 (m, 3H, ArH), 6.29 (s, 2H, ArH), 5.42 (s, 2H, CH_2), 3.81 (s, 3H, OCH_3), 3.57 (s, 9H, OCH_3), 2.40 (s, 3H, CH_3); ^{13}C NMR (100 MHz, DMSO-d_6) δ (ppm): 160.3, 153.0, 153.0, 140.8, 136.6, 136.1, 132.6, 131.7, 130.5, 130.5, 123.6, 122.6, 118.6, 114.2, 114.2, 113.4, 110.5, 103.6, 103.6, 59.9, 55.7, 55.7, 55.3, 47.3, 21.4; EIMS: *m/z* 418.0 (M^+); Anal. Calcd for $C_{25}H_{26}N_2O_4$: C, 71.75; H, 6.26; N, 6.69. Found: C, 71.58; H, 6.42; N, 6.55.

6.1.17. 6-Chloro-2-(4-methoxyphenyl)-1-(3,4,5-trimethoxybenzyl) benzimidazole (**17**)

Yield 68% from **6** as a pale-yellow solid, mp 92–93 °C; ^{1}H NMR (200 MHz, $CDCl_3$-d_1) δ (ppm): 7.71 (dd, $J=8$, 1 Hz, 1H, ArH), 7.62 (dd, $J=5$, 2 Hz, 2H, ArH), 7.26–7.20 (m, 2H, ArH), 6.96 (d, $J=8$ Hz, 2H, ArH), 6.25 (s, 2H, ArH), 5.30 (s, 2H, ArH), 3.83 (s, 3H, OCH_3), 3.82 (s, 3H, OCH_3), 3.70 (s, 3H, OCH_3); ^{13}C NMR (50 MHz, $CDCl_3$-d_1) δ (ppm): 161.2, 155.0, 153.9, 153.9, 141.8, 137.6, 136.8, 131.6, 130.6, 130.6, 128.5, 123.3, 121.9, 120.6, 114.4, 114.4, 110.3, 102.8, 102.8, 60.9, 56.2, 56.2, 55.4, 48.6; EIMS: *m/z* 438 (M^+); Anal. Calcd for $C_{24}H_{23}ClN_2O_4$: C, 65.68; H, 5.28; N, 6.38. Found: C, 65.62; H, 5.56; N, 6.28.

6.1.18. 5-Methyl-1-(3,4,5-trimethoxybenzyl)-2-(4-cyanophenyl) benzimidazole (**18**)

Yield 97% from **6** as a pale-red solid, mp 165–166 °C; ^{1}H NMR (400 MHz, DMSO-d_6) δ (ppm): 8.01 (d, $J=8$ Hz, 2H, ArH), 7.95 (d, $J=8$ Hz, 2H, ArH), 7.52–7.47 (m, 2H, ArH), 7.13 (d, $J=8$ Hz, 1H, ArH), 6.27 (s, 2H, ArH), 5.47 (s, 2H, CH_2), 3.57 (s, 9H, OCH_3), 2.42 (s, 3H, CH_3); ^{13}C NMR (100 MHz, dmso-d6) δ (ppm): 153.9, 153.5, 153.5, 151.8, 143.4, 137.3, 135.3, 134.8, 133.2, 133.2, 132.8, 132.2, 130.4, 130.4, 125.3, 119.7, 112.7, 111.4, 104.3, 104.3, 60.4, 56.3, 56.3, 48.2, 21.7; ESIMS: *m/z* 414 $(M+1)^+$; Anal. Calcd for $C_{25}H_{23}N_3O_3$: C, 72.62; H, 5.61; N, 10.16. Found: C, 72.70; H, 5.68; N, 10.02.

6.1.19. 2-(4-Fluorophenyl)-5-methyl-1-(3,4,5-trimethoxybenzyl) benzimidazole (**19**)

Yield 70% from **6** as a white solid, mp 132–133 °C; ^{1}H NMR (400 MHz, DMSO-d_6) δ (ppm): 7.77–7.75 (m, 2H, ArH), 7.56–7.53 (m, 2H, ArH), 7.48–7.45 (m, 2H, ArH), 7.07 (dd, $J=8$, 2 Hz, 1H, ArH), 6.28 (s, 2H, ArH), 5.44 (s, 2H, CH_2), 3.56 (s, 9H, OCH_3), 2.41 (s, 3H, CH_3); ^{13}C NMR (100 MHz, DMSO-d_6) δ (ppm): 153.6, 153.4, 153.4, 143.5, 134.5, 133.1, 131.7, 130.9, 130.5, 130.2, 129.7, 129.7, 129.4, 129.4, 124.6, 119.5, 111.2, 104.2, 104.2, 60.4, 56.2, 56.2, 48.0, 21.7; EIMS *m/z* 406 (M^+); Anal. Calcd for $C_{24}H_{23}FN_2O_3$: C, 70.92; H, 5.70; N, 6.89. Found: C, 70.87; H, 5.84; N, 6.82.

6.1.20. 2-(3-Methoxyphenyl)-5-methyl-1-(3,4,5-trimethoxybenzyl) benzimidazole (**20**)

Yield 88% from **6** as a white solid, mp 128–129 °C; ^{1}H NMR (400 MHz, $CDCl_3$-d_1) δ (ppm): 7.62 (s, 1H, ArH), 7.36–7.32 (m, 1H, ArH), 7.24–7.22 (m, 2H, ArH), 7.15(d, $J=8$ Hz, 1H, ArH), 7.07 (dd, $J=1$, 8 Hz, 1H, ArH), 7.01–6.98 (m, 1H, ArH), 6.28 (s, 2H, ArH), 5.33 (s, 2H, CH_2), 3.80 (s, 3H, OCH_3), 3.74 (s, 3H, OCH_3), 3.68 (s, 6H, OCH_3) 2.48 (s, 3H, CH_3); ^{13}C NMR (100 MHz, $CDCl_3$-d_1) δ (ppm): 159.8, 154.0, 153.8, 153.8, 143.4, 137.4, 134.3, 132.4, 132.3, 131.5, 129.8, 124.6, 121.4, 119.8, 116.3, 114.2, 109.9, 103.1, 103.1, 60.8, 56.1, 56.1, 55.3, 48.5, 21.6; EIMS: *m/z* 418 (M^+); Anal. Calcd for $C_{25}H_{26}N_2O_4$: C, 71.75; H, 6.26; N, 6.69. Found: C, 71.69; H, 6.39; N, 6.55.

6.1.21. 2-(3-Methylphenyl)-5-methyl-1-(3,4,5-trimethoxybenzyl) benzimidazole (**21**)

Yield 98% from **6** as a white solid, mp 137–138 °C; ^{1}H NMR (200 MHz, $CDCl_3$-d_1) δ (ppm): 7.60 (d, $J=6.92$ Hz, 2H, ArH), 7.43–7.24 (m, 3H, ArH), 7.16–7.03 (m, 2H, ArH), 6.28 (s, 2H, ArH), 5.32 (s, 2H, CH_2), 3.84 (s, 3H, OCH_3), 3.68 (s, 6H, OCH_3), 2.48 (s, 3H, CH_3), 2.37 (s, 3H, CH_3); ^{13}C NMR (50 MHz, $CDCl_3$-d_1) δ (ppm): 154.3, 153.7, 153.7, 143.5, 138.7, 138.7, 137.3, 134.2, 132.3, 132.3, 130.6, 130.2, 128.5, 126.0, 124.5, 119.7, 109.9, 103.0, 103.0, 60.8, 56.1, 56.1, 48.5, 21.6, 21.4; EIMS: *m/z* 402 (M^+); Anal. Calcd for $C_{25}H_{26}N_2O_3$: C, 74.60; H, 6.51; N, 6.96. Found: C, 74.72; H, 6.56; N, 6.89.

*6.1.22. 2-(3-Fluorophenyl)-5-methyl-1-(3,4,5-trimethoxybenzyl) benzimidazole (**22**)*

Yield 90% from **6** as a pink solid, mp 101–102 °C; ^{1}H NMR (400 MHz, DMSO-d_6) δ (ppm): 7.60–7.58 (m, 3H, ArH), 7.50–7.48 (m, 2H, ArH), 7.41–7.35 (m, 1H, ArH), 7.10 (dd, J = 8, 2 Hz, 1H, ArH), 6.29 (s, 2H, ArH), 5.47 (s, 2H, CH_2), 3.57 (s, 9H, OCH_3), 2.42 (s, 3H, CH_3); ^{13}C NMR (100 MHz, DMSO-d_6) δ (ppm): 163.7, 161.3, 153.5, 153.5, 143.3, 137.3, 134.6, 132.9, 131.9, 125.8, 124.9, 119.6, 117.2, 117.0, 116.6, 116.4, 111.3, 104.4, 104.4, 60.4, 56.2, 56.2, 48.1, 21.7; EIMS: m/z 406 (M^+); Anal. Calcd for $C_{24}H_{23}FN_2O_3$: C, 70.92; H, 5.70; N, 6.89. Found: C, 71.20; H, 5.76; N, 6.75.

*6.1.23. 2-(2-Methoxyphenyl)-5-methyl-1-(3,4,5-trimethoxybenzyl) benzimidazole (**23**)*

Yield 68% from **6** as a white solid, mp 194–195 °C; ^{1}H NMR (400 MHz, DMSO-d_6) δ (ppm): 7.55 (t, J = 8 Hz, 1H, ArH), 7.48 (dd, J = 8 Hz, 1H, ArH), 7.44–7.42 (m, 2H, ArH), 7.22 (d, J = 8 Hz, 1H, ArH), 7.11 (t, J = 8 Hz, 1H, ArH), 7.04 (d, J = 8 Hz, 1H, ArH), 6.27 (s, 2H, ArH), 5.15 (s, 2H, CH_2), 3.76 (s, 3H, OCH_3), 3.56 (s, 6H, OCH_3), 3.54 (s, 3H, OCH_3), 2.40 (s, 3H, CH_3); ^{13}C NMR (100 MHz, DMSO-d_6) δ (ppm): 157.4, 153.3, 153.3, 151.7, 142.6, 137.2, 133.6, 132.9, 132.7, 132.2, 131.2, 124.2, 121.2, 120.4, 119.3, 112.3, 110.9, 105.0, 105.0, 60.4, 56.2, 56.0, 56.0, 47.9, 21.6; EIMS: m/z 418 (M^+); Anal. Calcd for $C_{25}H_{26}N_2O_4$: C, 71.75; H, 6.26; N, 6.69. Found: C, 71.65; H, 6.35; N, 6.52.

*6.1.24. 2-(2-Methylphenyl)-5-methyl-1-(3,4,5-trimethoxybenzyl) benzimidazole (**24**)*

Yield 94% from **6** as a white solid, mp 160–166 °C; ^{1}H NMR (200 MHz, $CDCl_3$-d_1) δ (ppm): 7.60 (s, 1H, ArH), 7.41–7.28 (m, 4H, ArH), 7.24–7.19 (m, 1H, ArH), 7.08 (dd, J = 8, 1 Hz, 1H, ArH), 6.13 (s, 2H, ArH), 5.08 (s, 2H, CH_2), 3.75 (s, 3H, OCH_3), 3.65 (s, 6H, OCH_3), 2.48 (s, 3H, CH_3), 2.17 (s, 3H, CH_3); ^{13}C NMR (50 MHz, $CDCl_3$-d_1) δ (ppm): 153.4, 153.4, 143.4, 138.3, 137.4, 132.9, 132.1, 131.8, 130.5, 130.1, 130.1, 129.8, 125.7, 124.3, 119.8, 110.2, 109.8, 103.8, 103.8, 60.8, 56.0, 56.0, 48.0, 21.5, 19.7; EIMS: m/z 402 (M^+); Anal. Calcd for $C_{25}H_{26}N_2O_3$: C, 74.60; H, 6.51; N, 6.96. Found: C, 74.68; H, 6.59; N, 6.85.

*6.1.25. 2-(2-Chlorophenyl)-5-methyl-1-(3,4,5-trimethoxybenzyl) benzimidazole (**25**)*

Yield 24% from **6** as a pale-yellow solid, mp 174–175 °C; ^{1}H NMR (400 MHz, DMSO-d_6) δ (ppm): 9.66 (s, 1H, NH), 7.98 (d, J = 8 Hz, 2H, ArH), 7.56–7.49 (m, 3H, ArH), 7.26–7.13 (m, 5H, ArH), 7.03 (d, J = 8 Hz, 1H, ArH), 7.73–7.71 (m, 3H, ArH), 6.59 (dd, J = 8, 2 Hz, 1H, ArH), 5.33 (t, J = 6 Hz, 1H, NH), 4.24 (d, J = 6 Hz, 1H, CH_2), 3.75 (s, 6H, OCH_3), 3.71 (s, 3H, OCH_3); ^{13}C NMR (100 MHz, DMSO-d_6) δ (ppm): 166.2, 153.3, 153.3, 146.3, 144.8, 143.6, 136.6, 136.3, 135.1, 131.8, 128.7, 128.7, 128.3, 128.3, 127.3, 126.9, 126.6, 126.6, 122.6, 114.2, 110.0, 104.9, 104.9, 74.9, 60.2, 56.2, 56.2, 47.1, 21.2, 14.5; EIMS: m/z 422 (M^+); Anal. Calcd for $C_{24}H_{23}ClN_2O_3$: C, 68.16; H, 5.48; N, 6.62. Found: C, 68.26; H, 5.54; N, 6.55.

*6.1.26. 2-(2-Fluorophenyl)-5-methyl-1-(3,4,5-trimethoxybenzyl) benzimidazole (**26**)*

Yield 95% from **6** as a white solid, mp 93–95 °C; ^{1}H NMR (400 MHz, DMSO-d_6) δ (ppm): 7.68–7.62 (m, 2H, ArH), 7.52–7.37 (m, 4H, ArH), 7.10 (dd, J = 8, 2 Hz, 1H, ArH), 6.25 (s, 2H, ArH), 5.27 (s, 2H, CH_2), 3.57 (s, 3H, OCH_3), 3.55 (s, 6H, OCH_3), 2.41 (s, 3H, CH_3); ^{13}C NMR (100 MHz, DMSO-d_6) δ (ppm): 161.3, 158.9, 153.3, 153.3, 148.6, 143.6, 137.3, 133.7, 132.9, 132.8, 131.8, 125.5, 124.5, 119.6, 116.8, 116.6, 111.3, 104.7, 104.7, 60.2, 56.5, 56.5, 47.9, 21.6; EIMS: m/z 406 (M^+); Anal. Calcd for $C_{24}H_{23}FN_2O_3$: C, 70.92; H, 5.70; N, 6.89. Found: C, 70.84; H, 5.82; N, 6.81.

*6.1.27. 5-Methyl-2-(naphthalen-1-yl)-1-(3,4,5-trimethoxybenzyl) benzimidazole (**27**)*

Yield 95% from **6** as a white solid, mp 127–128 °C; ^{1}H NMR (400 MHz, DMSO-d_6) δ (ppm): 8.13 (d, J = 8 Hz, 1H, ArH), 8.04 (d, J = 8 Hz, 1H, ArH), 7.76 (t, J = 8 Hz, 2H, ArH), 7.67 (t, J = 8 Hz, 1H, ArH), 7.58–7.50 (m, 4H, ArH), 7.12 (d, J = 8 Hz, 1H, ArH), 6.10 (s, 2H, ArH), 5.22 (s, 2H, CH_2), 3.47 (s, 3H, OCH_3), 3.41 (s, 6H, OCH_3), 2.44 (s, 3H, CH_3); ^{13}C NMR (100 MHz, DMSO-d_6) δ (ppm): 153.2, 153.2, 152.1, 143.6, 137.1, 133.7, 133.6, 132.5, 132.2, 131.7, 130.6, 129.2, 128.9, 128.2, 127.6, 127.0, 125.8, 125.7, 124.6, 119.6, 111.3, 104.8, 104.8, 60.3, 56.0, 56.0, 47.9, 21.7; EIMS: m/z 438 $(M)^+$; Anal. Calcd for $C_{28}H_{26}N_2O_3$: C, 76.69; H, 5.98; N, 6.39. Found: C, 76.55; H, 6.12; N, 6.28.

*6.1.28. 5-Methyl-2-(naphthalen-2-yl)-1-(3,4,5-trimethoxybenzyl) benzimidazole (**28**)*

Yield 91% from **6** as a white solid, mp 123–124 °C; ^{1}H NMR (400 MHz, DMSO-d_6) δ (ppm): 8.33 (d, J = 2 Hz, 1H, ArH), 8.07 (d, J = 8 Hz, 1H, ArH), 8.00–7.79 (m, 2H, ArH), 7.89 (dd, J = 8, 2 Hz, 1H, ArH), 7.61–7.52 (m, 4H, ArH), 7.11 (d, J = 8 Hz, 1H, ArH), 6.30 (s, 2H, ArH), 5.54 (s, 2H, CH_2), 3.55 (s, 6H, OCH_3), 3.50 (s, 3H, OCH_3), 2.43 (s, 3H, CH_3); ^{13}C NMR (100 MHz, DMSO-d_6) δ (ppm): 153.1, 152.9, 152.9, 143.1, 136.7, 134.2, 133.0, 132.6, 132.5, 131.3, 128.8, 128.3, 128.3, 127.9, 127.6, 127.3, 126.8, 126.3, 124.2, 118.9, 110.7, 103.9, 103.9, 59.9, 55.6, 55.6, 47.6, 21.2; EIMS: m/z 438 (M^+); Anal. Calcd for $C_{28}H_{26}N_2O_3$: C, 76.69; H, 5.98; N, 6.39. Found: C, 76.53; H, 6.23; N, 6.22.

*6.1.29. 5-Methyl-2-styryl-1-(3,4,5-trimethoxybenzyl) benzimidazole (**29**)*

Yield 64% from **6** as a white solid, mp 160.5–165.1 °C; ^{1}H NMR (200 MHz, $CDCl_3$-d_1) δ (ppm): 7.95 (d, J = 16 Hz, 1H, CH), 7.57–7.49 (m, 3H, ArH), 7.35–7.32 (m, 3H, ArH), 7.20 (d, J = 16 Hz, 1H, CH), 7.13–6.99 (m, 2H, ArH), 6.31 (s, 2H, ArH), 5.35 (s, 2H, CH_2), 3.75 (s, 3H, OCH_3), 3.66 (s, 6H, OCH_3), 2.47 (s, 3H, CH_3); ^{13}C NMR (50 MHz, $CDCl_3$-d_1) δ (ppm): 153.7, 151.0, 143.5, 137.5, 137.2, 135.9, 133.7, 132.6, 131.8, 129.0, 129.0, 128.8, 128.5, 128.5, 127.2, 124.4, 119.2, 113.1, 109.0, 103.1, 103.1, 60.8, 56.1, 56.1, 47.0, 21.6; EIMS: m/z 414 (M^+); Anal. Calcd for $C_{26}H_{26}N_2O_3$: C, 75.34; H, 6.32; N, 6.76. Found: C, 75.22; H, 6.39; N, 6.47.

*6.1.30. 2-(3,4-Dichlorophenyl)-5-methyl-1-(3,4,5-trimethoxybenzyl) benzimidazole (**30**)*

Yield 68% from **6** as a white solid, mp 127–128 °C; ^{1}H NMR (400 MHz, DMSO-d_6) δ (ppm): 7.96 (d, J = 2 Hz, 1H, ArH), 7.79 (d, J = 8 Hz, 1H, ArH), 7.72 (dd, J = 8, 2 Hz, 1H, ArH), 7.52–7.50 (m, 2H, ArH), 7.11 (d, J = 8 Hz, 1H, ArH), 6.30 (s, 2H, ArH), 5.46 (s, 2H, CH_2), 3.58 (s, 9H, OCH_3), 2.42 (s, 3H, CH_3); ^{13}C NMR (50 MHz, $CDCl_3$-d_1) δ (ppm): 153.9, 153.9, 151.5, 143.2, 137.6, 134.5, 134.3, 133.1, 132.9, 131.8, 131.1, 130.7, 130.1, 128.1, 125.2, 119.9, 109.8, 102.9, 102.9, 60.9, 56.1, 56.1, 48.5, 21.6; EIMS: m/z 457 (M^+); Anal. Calcd for $C_{24}H_{22}Cl_2N_2O_3$: C, 63.03; H, 4.85; N, 6.13. Found: C, 62.89; H, 4.96; N, 6.01.

*6.1.31. 2-(2,4-Dichlorophenyl)-5-methyl-1-(3,4,5-trimethoxybenzyl) benzimidazole (**31**)*

Yield 35% from **6** as a pale-yellow solid, mp 148–149 °C; ^{1}H NMR (200 MHz, $CDCl_3$-d_1) δ (ppm): 7.61 (s, 1H, ArH), 7.53–7.52 (m, 1H, ArH), 7.33–7.32 (m, 2H, ArH), 7.19 (d, J = 8 Hz, 1H, ArH), 7.10 (dd, J = 8, 1 Hz, ArH), 6.11 (s, 2H, ArH), 5.12 (s, 2H, CH_2); ^{13}C NMR (50 MHz, $CDCl_3$-d_1) δ (ppm): 153.4, 153.4, 149.9, 143.3, 137.5, 136.8, 135.2, 133.0, 133.0, 132.4, 131.4, 129.8, 127.3, 125.0, 120.0, 110.0, 103.7, 103.7, 60.8, 56.0, 56.0, 48.4, 21.5; EIMS: m/z 457 (M^+); Anal. Calcd for $C_{24}H_{22}Cl_2N_2O_3$: C, 63.03; H, 4.85; N, 6.13. Found: C, 62.85; H, 4.94; N, 6.06.

*6.1.32. 2-(2,3-Dichlorophenyl)-5-methyl-1-(3,4,5-trimethoxybenzyl) benzimidazole (**32**)*

Yield 73% from **6** as a pale-yellow solid, mp 157–158 °C; ^{1}H NMR (400 MHz, DMSO-d_6) δ (ppm): 7.84 (dd, J = 8, 2 Hz, 1H, ArH), 7.60 (d, J = 2 Hz, 1H, ArH), 7.55–7.49 (m, 3H, ArH), 7.12 (d, J = 8 Hz, 1H, ArH), 6.24 (s, 2H, ArH), 5.19 (s, 2H, CH_2), 3.57 (s, 9H, OCH_3), 2.42 (s, 3H, CH_3); ^{13}C NMR (50 MHz, DMSO-d_6) δ (ppm): 153.4, 153.4, 150.4, 143.2, 137.5, 133.8, 132.9, 132.5, 132.4, 132.0, 131.3, 130.4, 127.5, 125.0, 120.1, 110.0, 103.8, 103.8, 102.9, 60.8, 56.0, 56.0, 48.4, 21.5; EIMS: m/z 457 (M^+); Anal. Calcd for $C_{24}H_{22}Cl_2N_2O_3$: C, 63.03; H, 4.85; N, 6.13. Found: C, 62.89; H, 4.96; N, 6.01.

*6.1.33. 2-(2,5-Difluorophenyl)-5-methyl-1-(3,4,5-trimethoxybenzyl) benzimidazole (**33**)*

Yield 74% from **6** as a white solid, mp 122–123 °C; ^{1}H NMR (400 MHz, DMSO-d_6) δ (ppm): 7.58–7.47 (m, 5H, ArH), 7.07 (dd, J = 8, 2 Hz, 1H, ArH), 6.28 (s, 2H, ArH), 5.44 (s, 2H, CH_2), 3.56 (s, 9H, OCH_3), 2.41 (s, 3H, CH_3); ^{13}C NMR (100 MHz, DMSO-d_6) δ (ppm): 153.6, 153.3, 153.3, 147.2, 143.5, 137.3, 133.7, 132.5, 131.9, 125.1, 119.7, 119.6, 119.4, 119.4, 119.2, 118.9, 111.4, 104.8, 104.8, 60.4, 56.2, 56.2, 48.0, 21.7; EIMS: m/z 424 (M^+); Anal. Calcd for $C_{24}H_{22}F_2N_2O_3$: C, 67.91; H, 5.22; N, 6.60. Found: C, 67.79; H, 5.38; N, 6.54.

*6.1.34. 2-(2,5-Difluorophenyl)-5-methyl-1-(3,4,5-trimethoxybenzyl) benzimidazole (**34**)*

Yield 61% from **6** as a white solid, mp 106–112 °C; ^{1}H NMR (200 MHz, $CDCl_3$-d_1) δ (ppm): 7.63 (d, J = 1 Hz, 1H, ArH), 7.45–7.41 (m, 1H, ArH), 7.18–6.98 (m, 4H, ArH), 6.19 (s, 2H, ArH), 5.15 (s, 2H, CH_2), 3.75 (s, 3H, OCH_3), 3.67 (s, 6H, OCH_3), 2.26 (s, 3H, CH_3); ^{13}C NMR (50 MHz, $CDCl_3$-d_1) δ (ppm): 158.7, 158.7, 153.5, 143.8, 142.8, 137.4, 133.0, 132.6, 132.4, 132.2, 131.3, 124.9, 120.1, 112.1, 111.6, 110.0, 104.1, 103.4, 103.4, 60.8, 55.9, 55.9, 48.3, 21.5; EIMS: m/z 424 (M^+); Anal. Calcd for $C_{24}H_{22}F_2N_2O_3$: C, 67.91; H, 5.22; N, 6.60. Found: C, 67.81; H, 5.35; N, 6.51.

6.2. Biological evaluation

6.2.1. Chemicals and reagents

Benzimidazole (BI), amoxicillin (AMX), clarithromycin (CLR), metronidazole (MTZ), gentamicin, and 3-[4,5-dimethylthiazol-2-yl]-2,5-diphenyl tetrazolium bromide (MTT) were purchased from Sigma–Aldrich (St. Louis, MO). Lipofectamine 2000 and F12 cell culture media were purchased from Invitrogen (Carlsbad, CA). β-Galactosidase expression vector, luciferase substrate (Promega, Madison, MA), fetal bovine serum (FBS, Gibco BRL, Grand Island, NY) were obtained from various suppliers. The NF-κB-luc promoter construct was kindly gifted from Dr. Chih-Hsin Tang (Department of Pharmacology, China Medical University) [30]. All other chemicals and reagents were of the highest grade commercially available and supplied either by Sigma–Aldrich or Merck (Whitehouse Station, NJ).

6.2.2. H. pylori strains

H. pylori, strain 26695 (ATCC 700392) was used as a reference strain as described previously [31]. The antibiotic resistant *H. pylori* strains, v633 and v1254, were clinical isolates, which were characterized as resistant to both metronidazole and clarithromycin as previously described [27]. *H. pylori* strains were routinely cultured on Brucella blood agar plates (Becton Dickinson, Franklin Lakes, NJ), containing 10% sheep blood under micro-aerophilic conditions at 37 °C for 48–72 h.

6.2.3. Determination of anti-H. pylori activity

The disk agar diffusion method was used to evaluate the anti-*H. pylori* activities of BI derivatives as described previously [31]. Four standard antimicrobial agents were used as positive controls, namely: benzimidazole (BI, 100 μg/mL), amoxicillin (AMX, 50 μg/mL), clarithromycin (CLR, 50 μg/mL), and metronidazole (MTZ, 800 μg/mL). While DMSO was used as a negative control.

6.2.4. Determination of minimum bactericidal concentration (MBC)

H. pylori strain 26695 and multidrug-resistant isolates were used to determine the MBC for BI and FMTMB using microdilution analysis at pH 5.0–8.0 as described previously [32]. The MBC is the lowest concentration of a tested sample that completely inhibits visible *H. pylori* growth on a Brucella blood agar plate.

6.2.5. Cell culture and cytotoxicity assay

Human gastric adenocarcinoma epithelial cells (AGS cells, ATCC CRL 1739) obtained from American Type Culture Collection (ATCC, Rockville, MD), were performed and cultured by a previously described method [31]. MTT assay was used to test the benzimidazole derivatives cytotoxicity toward AGS cells as described in our previous report [33].

6.2.6. Assays of H. pylori adhesion to and invasion into AGS cells

H. pylori invasion activity in AGS cells was investigated using a standard gentamicin assay as previously described [33]. Analyses of *H. pylori* anti-adhesion and anti-invasion of AGS cells were performed as previously reported [33]. The controls, containing *H. pylori*-infected AGS cells, without test samples, were used to define 100% adhesion or invasion. Results were expressed as the percentage of relative inhibition of *H. pylori* adhesion or invasion, by comparison with the controls.

6.2.7. Analysis of H. pylori-induced vacuolation of AGS cells

The vacuolation activity was determined by using neutral red uptake assay with slightly modification [19]. Briefly, AGS cells (0.5×10^5 cells) were cultured in 96-well microtiter plates for 24 h followed by infected with *H. pylori* strain 26695 at an MOI of 100. After 24 h incubation, the culture medium was removed and stained with 0.05% (w/v) neutral red (Sigma–Aldrich) for 5 min. The stained cells were then washed three times with PBS, and the neutral red was extracted using acidified alcohol. The levels of neutral red uptake was measured by a microplate ELISA reader (Biotek, Winooski, VT) at OD 540 nm. The control was a population of AGS cells without *H. pylori* infection or test sample present, and was used to define 100% cellular vacuolation. The results were expressed as the percentage of relative vacuole formation, by comparison with the control.

6.2.8. Analysis of cytotoxin-associated gene A (CagA) translocation and phosphorylation of AGS cells

The preparation of immunoprecipitates for analysis of *H. pylori* translocated and phosphorylated CagA was described in our previous report [34]. The immunoprecipitates were then subjected to 6.5% SDS-PAGE and transferred onto polyvinylidene difluoride (PVDF) membrane (Pall, East Hills, NY) for immunoblot analysis. CagA was probed with mouse anti-CagA antibody (Santa Cruz Biotechnology); tyrosine-phosphorylated CagA was probed with mouse anti-phosphotyrosine antibody (4G10) (Upstate Biotechnology, Billerica, MA). To ensure equal loading of each prepared sample, actin from whole-cell lysates, was stained using goat anti-actin antibody (Santa Cruz Biotechnology). The proteins of interest were visualized using enhanced chemiluminescence reagents (GE Healthcare, Buckinghamshire, UK) and were detected by exposure to X-ray film (Kodak, Boca Raton, FL, USA).

6.2.9. Assessment of H. pylori-induced hummingbird phenotype of AGS cells

AGS cells (1×10^6 cells) were cultured in 12-well plates at 37 °C for 24 h followed by infection with *H. pylori* strain 26695 at a MOI of 50 for 6 h. Elongated cells (hummingbird phenotype) were defined as cells that had thin needlelike protrusions that were greater than 20 μm long, and presented a typical elongated shape as described by our previous report [34]. All samples were determined in duplicate from three independent experiments. The proportion of elongated cells was calculated from the numbers of *H. pylori*-infected cells having the hummingbird phenotypes.

6.2.10. Transient transfection of NF-κB reporter and measurement of IL-8

The analysis of NF-κB reporter luciferase activity and measurement of IL-8 expression have been described in our previous reports [32,33].

6.2.11. Statistical analysis

Student's *t*-test was used to calculate the statistical significance of experimental results between two groups. Differences in data values were considered significant at $^*P < 0.05$.

Acknowledgments

This study was supported by the National Science Council of Taiwan (NSC98-2320-B-039-007-MY3, NSC99-2815-C-039-050-B, NSC100-2313-B-039-003), by China Medical University (CMU97-346, CMU98-S-09, CMU98-S-38), and by Tomorrow Medical Foundation. We thank Yen-Ru Chen (National Chung Hsing University) for expert technical assistance. This study was supported in part by the Taiwan Department of Health Clinical Trial and Research Center of Excellence (DOH101-TD-B-111-004).

Supplementary data

Supplementary data associated with this article can be found in the online version, at doi:10.1016/j.ejmech.2011.12.021. These data include MOL files and InChiKeys of the most important compounds described in this article.

References

[1] H. Miyaji, T. Azuma, S. Ito, Y. Abe, F. Gejyo, N. Hashimoto, H. Sugimoto, H. Suto, Y. Ito, Y. Yamazaki, Y. Kohli, M. Kuriyama, J. Gastroenterol. Hepatol. 15 (2000) 257–262.
[2] K.J. Goodman, P. Correa, Lancet 355 (2000) 358–362.
[3] C. Montecucco, R. Rappuoli, Nat. Rev. Mol. Cell Biol. 2 (2001) 457–466.
[4] E.J. Kuipers, Aliment. Pharmacol. Ther. 13 (Suppl. 1) (1999) 3–11.
[5] A. Covacci, J.L. Telford, G. Del Giudice, J. Parsonnet, R. Rappuoli, Science 284 (1999) 1328–1333.
[6] R.J. Hopkins, L.S. Girardi, E.A. Turney, Gastroenterology 110 (1996) 1244–1252.
[7] R.W. Van der Hulst, E.A. Rauws, B. Koycu, J.J. Keller, M.J. Bruno, J.G. Tijssen, G.N. Tytgat, Gastroenterology 113 (1997) 1082–1086.
[8] R.P. Logan, P.A. Gummett, J.J. Misiewicz, Q.N. Karim, M.M. Walker, J.H. Baron, Lancet 338 (1991) 1249–1252.
[9] E. Hentschel, G. Brandstatter, B. Dragosics, A.M. Hirschl, H. Nemec, K. Schutze, M. Taufer, H. Wurzer, N. Engl. J. Med. 328 (1993) 308–312.
[10] J. Tankovic, D. Lamarque, C. Lascols, C.J. Soussy, J.C. Delchier, Pathol. Biol. (Paris) 49 (2001) 528–533.
[11] S.K. Poon, C.S. Chang, J. Su, C.H. Lai, C.C. Yang, G.H. Chen, W.C. Wang, Aliment. Pharmacol. Ther. 16 (2002) 291–296.
[12] F. Megraud, H. Lamouliatte, Aliment. Pharmacol. Ther. 17 (2003) 1333–1343.
[13] E.M. Muri, J.S. Williamson, Mini Rev. Med. Chem. 4 (2004) 201–206.
[14] D. Carcanague, Y.K. Shue, M.A. Wuonola, M. Uria-Nickelsen, C. Joubran, J.K. Abedi, J. Jones, T.C. Kuhler, J. Med. Chem. 45 (2002) 4300–4309.
[15] E. Iwao, K. Yamamoto, Y. Yokoyama, F. Hirayama, K. Haga, J. Infect. Chemother. 10 (2004) 90–96.
[16] S.D. Mills, W. Yang, K. MacCormack, Antimicrob. Agents Chemother. 48 (2004) 2524–2530.
[17] M.R. Amieva, E.M. El-Omar, Gastroenterology 134 (2008) 306–323.
[18] N. Figura, P. Guglielmetti, A. Rossolini, A. Barberi, G. Cusi, R.A. Musmanno, M. Russi, S. Quaranta, J. Clin. Microbiol. 27 (1989) 225–226.
[19] T.L. Cover, W. Puryear, G.I. Perez-Perez, M.J. Blaser, Infect. Immun. 59 (1991) 1264–1270.
[20] M. Stein, R. Rappuoli, A. Covacci, Proc. Natl. Acad. Sci. USA 97 (2000) 1263–1268.
[21] S. Brandt, T. Kwok, R. Hartig, W. Konig, S. Backert, Proc. Natl. Acad. Sci. USA 102 (2005) 9300–9305.
[22] J. Sheng, P.T. Nguyen, J.D. Baldeck, J. Olsson, R.E. Marquis, Arch. Oral Biol. 51 (2006) 1015–1023.
[23] P.T. Nguyen, J.D. Baldeck, J. Olsson, R.E. Marquis, Oral Microbiol. Immunol. 20 (2005) 93–100.
[24] L. Olbe, E. Carlsson, P. Lindberg, Nat. Rev. Drug Discov. 2 (2003) 132–139.
[25] W.L. Chang, C.S. Chang, P.C. Chiang, Y.F. Ho, J.F. Liu, K.W. Chang, J.H. Guh, Br. J. Pharmacol. 160 (2010) 1677–1689.
[26] N. Vakil, F. Megraud, Gastroenterology 133 (2007) 985–1001.
[27] C.H. Lai, C.H. Kuo, P.Y. Chen, S.K. Poon, C.S. Chang, W.C. Wang, J. Antimicrob. Chemother. 57 (2006) 466–471.
[28] M. Marchetti, B. Arico, D. Burroni, N. Figura, R. Rappuoli, P. Ghiara, Science 267 (1995) 1655–1658.
[29] N.R. Salama, G. Otto, L. Tompkins, S. Falkow, Infect. Immun. 69 (2001) 730–736.
[30] Y.C. Fong, M.C. Maa, F.J. Tsai, W.C. Chen, J.G. Lin, L.B. Jeng, R.S. Yang, W.M. Fu, C.H. Tang, J. Bone Miner. Res. 23 (2008) 961–970.
[31] C.H. Lai, S.H. Fang, Y.K. Rao, M. Geethangili, C.H. Tang, Y.J. Lin, C.H. Hung, W.C. Wang, Y.M. Tzeng, J. Ethnopharmacol. 118 (2008) 522–526.
[32] C.H. Lai, Y.K. Rao, S.H. Fang, Y.T. Sing, Y.M. Tzeng, Bioorg. Med. Chem. Lett. 20 (2010) 5462–5465.
[33] M. Geethangili, S.H. Fang, C.H. Lai, Y.K. Rao, H.M. Lien, Y.M. Tzeng, Food Chem. 119 (2010) 149–153.
[34] C.H. Lai, Y.C. Chang, S.Y. Du, H.J. Wang, C.H. Kuo, S.H. Fang, H.W. Fu, H.H. Lin, A.S. Chiang, W.C. Wang, Infect. Immun. 76 (2008) 3293–3303.